Technology in Cancer Research & Treatment
2017, Vol. 16(6) 1113–1119

DOI: 10.1177/1533034617734689
journals.sagepub.com/home/tct
SAGE

Dosimetric Analysis of Microscopic Disease in SBRT for Lung Cancers

Ronghu Mao, MD[1], Lingling Tian, MD[1], You Zhang, PhD[2], Lei Ren, PhD[2], Renqi Gao, PhD[2], Fang-Fang Yin, PhD[2], and Hong Ge, PhD[1]

Abstract

Objective: The objective of this study is to theoretically and experimentally evaluate the dosimetry in the microscopic disease regions surrounding the tumor under stereotactic body radiation therapy of lung cancer. **Methods:** For simplicity, the tumor was considered moving along 1 dimension with a periodic function. The probability distribution function of the tumor position was generated according to the motion pattern and was used to estimate the delivered dose in the microscopic disease region. An experimental measurement was conducted to validate both the estimated dose with a probability function and the calculated dose from 4-dimensional computed tomography data using a dynamic thorax phantom. Four tumor motion patterns were simulated with $\cos^4(x)$ and sin(x), each with 2 different amplitudes: 10 mm and 5 mm. A 7-field conformal plan was created for treatment delivery. Both films (EBT2) and optically stimulated luminescence detectors were inserted in and around the target of the phantom to measure the delivered doses. Dose differences were evaluated using gamma analysis with 3%/3 mm. **Results:** The average gamma index between measured doses using film and calculated doses using average intensity projection simulation computed tomography was 80.8% $\pm$ 0.9%. In contrast, between measured doses using film and calculated doses accumulated from 10 sets of 4-dimensional computed tomography data, it was 98.7% $\pm$ 0.6%. The measured doses using optically stimulated luminescence detectors matched very well (within 5% of the measurement uncertainty) with the theoretically calculated doses using probability distribution function at the corresponding position. Respiratory movement caused inadvertent irradiation exposure, with 70% to 80% of the dose line wrapped around the 10 mm region outside the target. **Conclusion:** The use of static dose calculation in the treatment planning system could substantially underestimate the actual delivered dose in the microscopic disease region for a moving target. The margin for microscopic disease may be substantially reduced or even eliminated for lung stereotactic body radiation therapy.

Keywords

microscopic disease, 4DCT, probability distribution function, lung SBRT, target motion

Abbreviations

AIP, average intensity projection; BED, biological equivalent dose; CTV, clinical target volume; 4DCT, 4-dimensional computed tomography; GTV, gross tumor volume; IID, inadvertent irradiation doses; ITV, internal target volume; MD, microscopic disease; MIP, maximum intensity projection; MUs, monitor units; OSLDs, optically stimulated luminescence detectors; PDF, probability density function; PTV, planning target volume; RPM, real-time position management; SBRT, stereotactic body radiation therapy; SI, superior–inferior; TPS, treatment planning system

Received: February 15, 2017; Revised: July 12, 2017; Accepted: September 1, 2017.

Introduction

Stereotactic body radiation therapy (SBRT) of lung cancer requires a precise delineation of the target volume for minimizing the pulmonary toxic effects by reducing the normal lung tissue in the planning target volume (PTV). On the other hand, the respiratory-associated movement of the target

[1] Department of Radiation Oncology, Henan Cancer Hospital, The Affiliated Cancer Hospital of Zhengzhou University, Henan, China
[2] Department of Radiation Oncology, Duke University Medical Center, Durham, NC, USA

Corresponding Author:
Hong Ge, PhD, Department of Radiation Oncology, Henan Cancer Hospital, The Affiliated Cancer Hospital of Zhengzhou University, 127 Dongming Rd, Zhengzhou, Henan 450008, China.
Email: gehong666@126.com

volume may lead to underdosing of the target volume if sufficient margin is not given to the clinical target volume (CTV) and may result in unmatched delivery dose with the prescription dose.[1] Potentially, this may affect the treatment outcomes. Therefore, understanding the influence of respiratory motion on the dosimetry, especially in the margin region from gross tumor volume (GTV) to CTV, is the key for radiation therapy of lung cancers.

Conventionally, we design treatment plans based on target volumes delineated using the maximum intensity projection (MIP), which was calculated from 4-dimensional computed tomography (4DCT) for free-breathing treatment. In recent years, many respiratory motion management techniques have been developed to minimize the normal lung volume in the PTV, such as breath-holding, respiratory gating, and real-time tracking using multiple leaf collimator.[2] However, these techniques have their corresponding limitations, and some of them are still at the development stage. Although both breath-holding[3] and respiratory gating[4,5] could potentially reduce the irradiated normal tissue volume by reducing the margin required from CTV to PTV, they usually require complicated implementation procedures with increased treatment time. In addition, patients with poor pulmonary functions usually have difficulties in breath-holding. The effectiveness of respiratory gating technique is also limited as tumor motion during the course of treatment can be different from planning and simulation. In comparison, the conventional free-breathing treatment is more convenient than those using respiratory management techniques,[6,7] since it does not need additional efforts from the patients or implementations of additional hardware and software. However, the free-breathing plans usually require the delineation of a larger PTV and will introduce higher dose to the normal tissues. Therefore, it is important to investigate how PTV volume could be minimized when applying free-breathing treatment. Traditionally, PTV includes margins from GTV to CTV, CTV to internal target volume (ITV), and ITV to PTV. The margins for CTV and ITV are often complicated as the distribution of microscopic disease (MD) and target motion are not easily determined. It is not clear whether the margin required to include MD could be reduced or ignored when motion-related margin is added.

This study aims to analyze the dosimetric impact from respiration-associated target motion for radiation therapy of lung cancers, especially in the MD region. Better understanding of the dosimetric patterns of a moving target may guide better delineation of targets in free-breathing plans and potentially reduce the normal tissue dose by minimizing the margin from GTV to CTV. In this study, we designed PTV by removing the margin for MD between GTV and CTV to investigate the incident rate of the respiration-associated MD region inside the ITV during the irradiation period using a probability density function (PDF). We anticipate that with the current free-breathing dose delivery technique, some inadvertent irradiation doses (IID) will also be delivered to the MD region, which may be enough to control MD even without adding MD margin between GTV and CTV, that is, defining ITV directly from GTV.

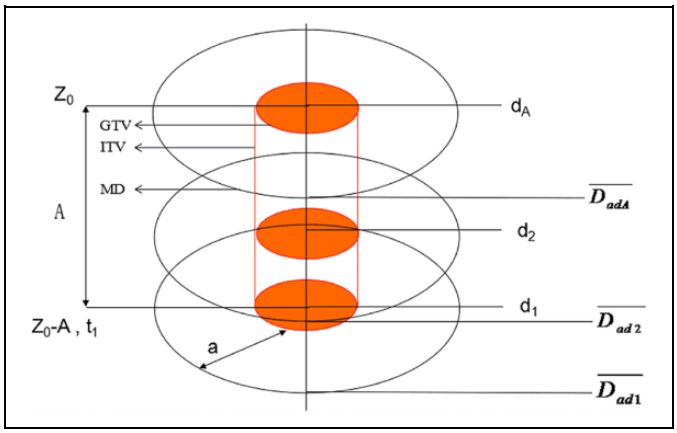

Figure 1. Microscopic disease was surrounding the target (GTV). It would appear at different locations within ITV in different respiratory phases. The MD region received the average doses at different phases. Here *a* represents the extension location of MD around GTV. GTV indicates gross target volume; ITV, internal target volume; MD, microscopic disease.

Methods and Materials

Several studies have noted that lung respiratory motion was predominant (though not exclusively) in the patient superior–inferior (SI) direction.[8,9] Thus, for simplicity, we assumed in this study that (1) the organ motion was uniform along 1-dimensional (SI) direction and (2) the anatomical structures (both tumor and MD) were rigid with no deformation.

Probability Density Function

For the respiratory motion with a fixed period, the position of the target as a function of time can be parameterized by the following equation[10]:

$$Z(\mathrm{t}) = Z_0 - A\cos^{2n}\left(\frac{\pi t}{T} - \varphi\right), \quad (1)$$

where $Z(t)$ denotes the target position at time t, Z_0 denotes the target position at the peak-expiration phase, A denotes the amplitude (extent) of motion, $(Z_0 - A)$ denotes the target position at the peak-inspiratory phase, n denotes the degree of asymmetry, T denotes the period of motion, φ denotes the starting phase of the breathing cycle, and d denotes the motion displacement from the initial position, such as $d_1, d_2, \ldots, d_A$, as shown in Figure 1. Here the target means GTV.

Assume that the center of the target at the peak-inspiration is at position $Z = Z_0 - A$ at time $t = t_1$,

$$Z_0 - A = Z_0 - A\cos^{2n}\left(\frac{\pi t_1}{T} - \varphi\right). \quad (2)$$

And assume that the center of the target is at position $Z = Z_0 - A + d$ at time $t = t_d$,

$$Z_0 - A + d = Z_0 - A\cos^{2n}\left(\frac{\pi t_d}{T} - \varphi\right). \quad (3)$$

We can then obtain t_1 and t_d from Equations 2 and 3, respectively:

$$t_1 = \frac{T\varphi}{\pi}, t_d = \frac{T}{\pi}\left[\varphi + \cos^{-1}\left(1 - \frac{d}{A}\right)^{\frac{1}{2n}}\right]. \quad (4)$$

The corresponding PDF, defined as the appearance of the interested region between the time interval of $(t_{d+1} - t_d)$ in the treatment field during the period of T, is as follows:

$$P_d = \frac{[(t_{d+1} - t_1) - (t_d - t_1)] \times 2}{T} \times 100\%. \quad (5)$$

Equation 5 can transformed to Equation 6 using information in Equation 4:

$$P_d = \frac{2}{\pi} \times \left\{\cos^{-1}\left(1 - \frac{d+1}{A}\right)^{\frac{1}{2n}} - \cos^{-1}\left(1 - \frac{d}{A}\right)^{\frac{1}{2n}}\right\}. \quad (6)$$

Dose Estimation in MD Region Based on PDF

Based on the derived motion PDF and the initial dose distribution calculated from the treatment plan using the average intensity projection (AIP) CT data set, the dose in the MD region with a defined margin a from the GTV edge, as shown in Figure 1, could be estimated as follows:

$$D_a = \overline{D_{ad1}}P_{ad1} + \overline{D_{ad2}}P_{ad2} + \overline{D_{ad3}}P_{ad3} + \ldots + \overline{D_{adA}}P_{adA}. \quad (7)$$

We divided the MD region into narrow bands with a step size of 1 mm. The average doses in these divided bands were represented by $\overline{Dad1}, \overline{Dad2}, \overline{Dad3}, \ldots \overline{DadA}$. $Pad1, Pad2, Pad3, \ldots PadA$ are the relative weightings of each phase determined by the time spent in each phase as calculated using Equation 6, where $P\text{ad}1 + P\text{ad}2 + P\text{ad}3 + \ldots + P\text{ad}A = 1$.

Phantom Study

A CIRS Dynamic Thorax Phantom (Model 008A; Computerized Imaging Reference Systems, Norfolk, Virginia) with a 3-cm spherical moving insert (as tumor) was used in the phantom study. CIRS motion control software was used to drive tumor motion with different breathing patterns. Motion curves using both cos4(x) and sin(x) patterns with 2 different amplitudes of 5 mm and 10 mm for each pattern were used. For each breathing pattern, a 4DCT scan was performed on a 4-slice clinical CT scanner (Lightspeed; GE Healthcare, Milwaukee, Wisconsin). The real-time position management (RPM) system (Varian Medical Systems, Palo Alto, California) was used to track the respiratory motion. The following imaging parameters were used: 120 kV, 290 mA, and 2.5-mm slice thickness. The acquired images were retrospectively sorted using the Advantage 4D software (GE Health care), with respiratory phases determined from the RPM signal to generate 10-phase 4DCT image data sets. Both MIP and AIP data sets were calculated using all 10 phases of the 4DCT. The

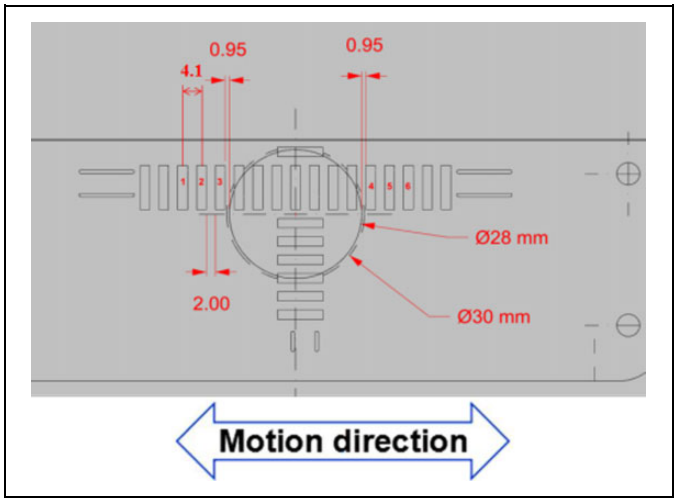

Figure 2. Illustration of point dose measurements using the OSLDs which were placed in the small rectangular boxes in the phantom. The point dose locations (labeled as 1 to 6 along the motion direction) were selected for OSLDs measurements. The distance between measurement points is 4.1 mm. No OSLDs were placed in the perpendicular direction. The circle represents the GTV with a diameter of 3 cm. The film was placed on the top of this drawing to cover the full range of the motion.[12] GTV indicates gross target volume; OSLDs, optically stimulated luminescence detectors.

MIP, AIP, and all 10 individual 4DCT phase images were sent to a treatment planning system (TPS, Eclipse, version 13.6; Varian Medical Systems, Inc) for contouring, planning, and dose calculation.

Treatment Planning

From the imported CT images, both ITV and PTV were contoured according to a clinical protocol used for lung SBRT patients. First, we manually contoured the target (GTV) on the MIP CT data set to identify the ITV. In this process, we set GTV = CTV and did not add a margin for MD to GTV. The MIP-derived ITV was expanded by a uniform 5-mm margin to create a PTV. A 7-field 3D conformal plan with 6 MV photon beams was created on the AIP image using the MIP-derived PTV. Three Gy was prescribed for each plan with a dose rate of 100 monitor units (MUs) per minute, covering 15 breathing cycles per treatment delivery. Three Gy was selected to account for the dose characteristics of the film.[11] The dose distribution was calculated using the Analytical Anisotropic Algorithm with a grid size of 2 mm and heterogeneity correction. The ITV obtained from the 4DCT image data was actually the GTV boundary trajectory. As the MD was presumably distributed surrounding the target (GTV), it would therefore appear at different locations within ITV in different respiratory phases.

Four-Dimensional Planned Dose Distribution of Motion

To create the full 4D dose distribution, we generated 10 plans using 10-phase CT data sets by copying the AIP plan to each phase of the 4DCT image data sets. The planning parameters

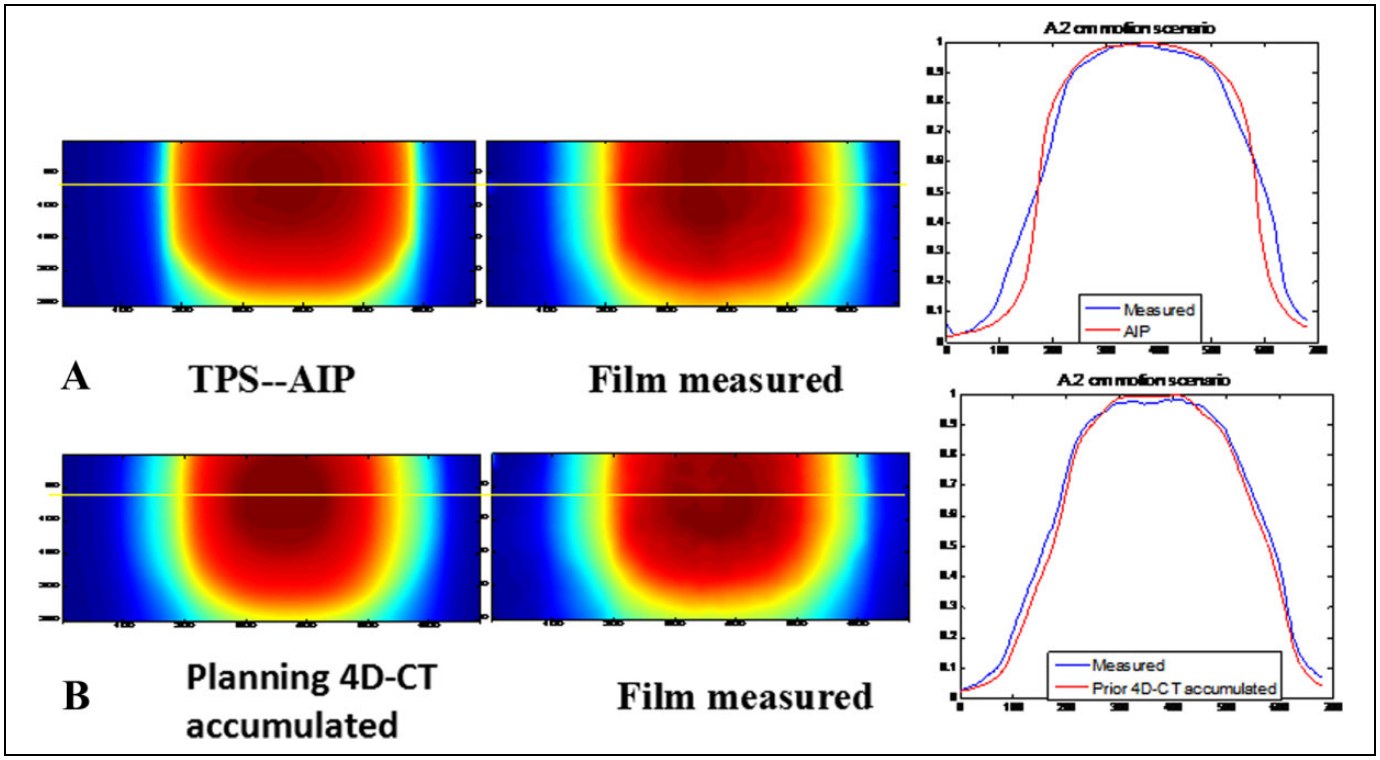

Figure 3. Dose distributions and profile comparison between (A) EBT2 film–measured dosimetry and calculated AIP planned dosimetry and (B) EBT2 film–measured dosimetry and 4DCT accumulated dosimetry using cos4(x) breathing pattern with a motion amplitude of 10 mm. (The profile locations are indicated with white lines in the figures.) AIP indicates average intensity projection; 4DCT, 4-dimensional computed tomography.

(leaf positions and beam arrangement) remained unchanged except for the MU, which was scaled down by a factor of 1/10. In total, 10 dosimetric maps were obtained. The dose calculated from one of the phase plans (in this study, 60% phase data set) was used as the reference dose distribution. Doses calculated from other phase plans were superimposed on this reference dose plan for summation using a MATLAB program through a rigid registration of the target.

Dose Comparison

Both EBT2 films (Gafchromic EBT; International Specialty Products, Wayne, New Jersey) and optically stimulated luminescence detectors (OSLDs) were inserted in and around the target of the motion phantom to measure the dose during radiation delivery using a TrueBeam machine (Varian Medical Systems). The OSLDs and the film were placed inside the movable rod of the phantom for actual target dose measurement and the film was placed in between the 2 halves of the tumor.[12] Figure 2 illustrates some of the selected dose measurement locations of 1 to 6. The distance between points is 4.1 mm.

Both point doses measured using OSLDs and 2D planar doses measured using Radiochromic EBT2 films were compared to the doses from the TPS. Optically stimulated luminescence detectors were used to assess absolute dosimetry inside and outside the GTV. The percentage dose discrepancy was defined as (calculated − measured)/measured. Radiochromic film was used to evaluate the relative spatial dosimetry. The irradiated films were digitized, converted to the dose, and registered with the corresponding planned dose distributions from the TPS.[12] The dose uncertainty of each film measurement was around 3.5%.[13] The passing γ criteria were set at ±3% of the normalization dose or 3 mm distance to agreement (3%/3 mm). Data were analyzed statistically using the SPSS 17.0.

Table 1. Gamma Indices (3 mm/3%) Computed Between Film-Measured Dose and 4DCT Accumulated Dose and Between Film-Measured Dose and AIP Planned Dose.[a]

		Gamma Pass Rate (3%/3 mm)	
Motion Curve	Amplitude (mm)	4D Dose vs Film Dose	AIP Planned Dose vs Film Dose
cos4(x)	10	98.9%	80.6%
cos4(x)	5	98.7%	79.8%
sin(x)	10	97.8%	80.9%
sin(x)	5	99.3%	82.1%
Mean		98.67%	80.85%
Standard deviation		±0.63%	±0.95%

Abbreviations: AIP, average intensity projection; 4DCT, 4-dimensional computed tomography.
[a]The results were grouped by motion curve, amplitude, and dose calculation methods.

Table 2. Comparison Between OSLD Measured Doses and Theoretically Calculated Doses, With Motion Amplitudes of 10 mm and 5 mm for cos4(x) Curve and sin(x) Curves.[a]

			Dose Comparison at Different Measurement Positions					
Curve	Amplitude (mm)	Dose (cGy)	10 mm	6 mm	2 mm	−2 mm	−6 mm	−10 mm
Cos4(x)	10	Calculated	308.9	325.3	334.2	323.1	306.2	264.9
		Measured	303.6	311.4	321.6	320.6	311.8	265.2
		% diff	1.7	4.5	3.9	0.8	−1.8	−0.1
Cos4(x)	5	Calculated	265.8	307	326.7	315.6	302.3	252.6
		Measured	254.1	301.1	321.7	326	299.8	252.2
		% diff	4.6	2.0	1.6	-3.2	0.8	0.2
Sin(x)	10	Calculated	304.7	322	331.96	333.6	324.6	308.6
		Measured	280.8	315.2	325.4	330.2	313.6	296.6
		% diff	8.5	2.2	2.0	1.0	3.5	4.0
Sin(x)	5	Calculated	242.2	298	323.2	327.7	309.5	266.8
		Measured	256.5	297.9	314.4	310.9	302.9	254.2
		% diff	−5.6	0.0	2.8	5.4	2.2	5.0

Abbreviation: OSLD, optically stimulated luminescence detector.
[a]Measurement points within internal target volume (ITV) are defined as positive and out of ITV as negative. 0 represents the edge of ITV.

Results

Film Results

Figure 3 shows a profile comparison between EBT2 film dosimetry and AIP planned dosimetry and between EBT2 film-measured dosimetry and 4DCT accumulated dosimetry using cos4(x) breathing pattern with an amplitude of 10 mm. A dose profile comparison between the film-measured doses and the AIP doses illustrated the disagreement at the beam penumbra region. In contrast, the 4D accumulated dose profiles showed good agreement with the measured profiles at regions both inside and outside of the target.

Table 1 shows the percentage of pixels (gamma index) passing the 3%/3 mm criteria. The average gamma indices for 4D accumulated doses and the AIP doses were 98.7% ± 0.6% and 80.8% ± 0.9%, respectively.

Optically Stimulated Luminescence Detector Results

Table 2 compares OSLD measured doses to theoretically calculated doses based on the PDF using Equation 7, with motion amplitudes of 10 and 5 mm and breathing patterns of cos4(x) curve and sin(x) curves. Theoretically calculated dose values were very close to the measured doses of OSLDs, especially for areas near the GTV boundary.The dose fall-off curves for different motion amplitudes were calculated in both sin(x) curve and cos4(x) curve (Figure 4). The doses at the locations between 6 and 9 mm outside GTV still had approximately 80% of the prescription dose coverage, with the penalty of having relatively nonuniform dose distribution both inside and outside the PTV. Considering that the GTV-to-CTV margin is usually 6 to 8 mm for lung cancers,[14] this result demonstrates that if the respiratory motion and its PDF are known in advance under the conditions that we assumed in this study, we can use them to substantially reduce the MD margin and thus the dose to the normal tissue, while maintaining GTV and MD dose coverage.

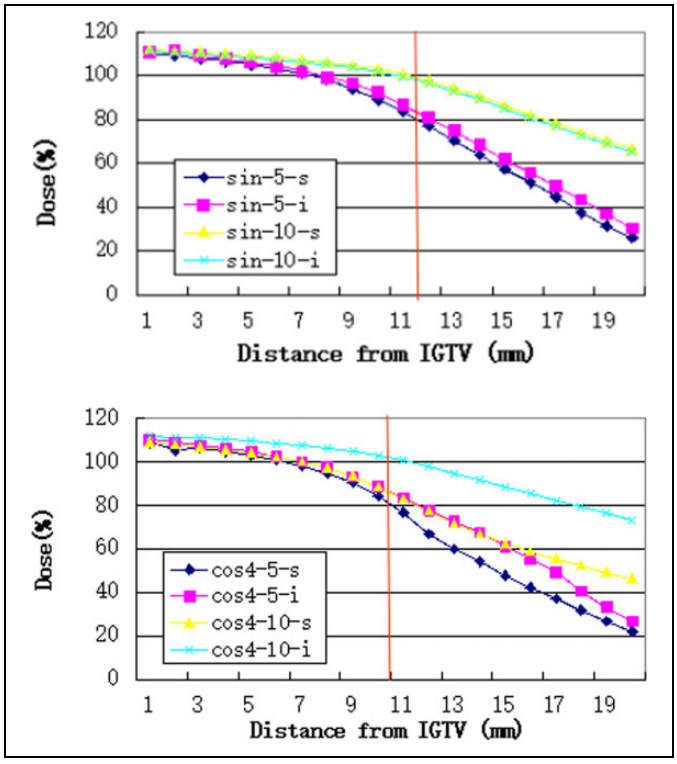

Figure 4. Dose fall-off for different motion amplitudes of sin(x) curve and cos4(x) curve; 70% to 80% of the dose line can be wrapped around the 10 mm region outside the target. The sin-5-s indicates sin(x) curve in the superior direction with motion amplitude of 5 mm. The sin-5-i indicates the sin(x) curve in the inferior direction with motion amplitude of 5 mm.

Discussion

Although current imaging techniques adequately revealed GTV and ITV,[15-17] they cannot show the MD around the target (GTV). The movement of MD is virtually unknown through the

existing imaging technology. At present, the range of GTV to CTV is mainly created based on physicians' knowledge and experience as well as the biological characteristics of tumor. In lung squamous cell carcinoma, a 6-mm GTV margin is typically used for MD. For adenocarcinoma, a 8-mm GTV margin is typically used for MD.[18-20]

In this study, the target volumes (GTV, CTV, ITV, and PTV) were considered as static and independent in International Commission on Radiation Units and Measurements Report 62[21] during the course of irradiation, although the MD region was appeared in different positions in ITV due to respiratory motion. Such an assumption could not accurately reflect dose discrepancy caused by the movement of the target, the MD region, and the normal surrounding tissues. At present, there was no reported actual MD dosimetry. We first reported the estimated MD dosimetry using a mathematical model (PDF) and validated its accuracy through measurements. Our study also indicated that the static dose distribution of MD displayed in the TPS was deviated from the actual dose due to the target movement. The TPS may considerably underestimate the actual dose in the MD region. The MD will move into the center of the treatment field during respiration, which receives more dose than that assumed by the static approach. Based on our results from 4DCT dose accumulation and 1D motion probability dose estimation, we found that locations with 10 mm outside the target (GTV) still received around 70% to 80% of the prescription dose even without margin for MD.

This study fully used the respiration-associated target motion characteristics of lung cancer to theoretically estimate the probability of MD region inside the ITV as well as MD dosimetry during the irradiation period. The currently existing 3D TPS was not able to directly calculate actual cumulative dose distribution of the motion target. The results obtained from this study may be used to determine the amount of margin needed for MD, especially for large fractional doses and biologically equivalent doses of SBRT.

For subclinical disease, the prevailing consensus is that the dose necessary for effective radiotherapy is approximately 45 to 50 Gy. It is reasonable to assume that a dose of 50 Gy in 2 Gy per fraction is necessary to achieve an overall 90% reduction in the incidence of metastases.[22] When the clinical SBRT prescription dose is 50 Gy in 5 fractions and a conventional formula biological equivalent dose (BED) $= nd \times (1 + d/[\alpha/\beta])$ is used, the BED to GTV is approximately 100 Gy. A region with 10 mm expansion from the ITV will approximately receive 80% of the prescription dose, which will equivalently be BED of 80 Gy, far greater than 50 Gy. We would then consider that the MD region was able to achieve sufficient BED without expanding the CTV margin for MD. As a result, the dose to normal lung tissue will be substantially reduced.

In this study, we demonstrated that the dose in the MD region was affected by respiratory motion and SBRT BED in free-breathing treatment. From the dosimetric point of view, we may be able to substantially reduce or even eliminate the margin needed to account for MD for lung SBRT to achieve the anticipated curative effect, resulting in a substantial dose reduction in the normal lung dose. It may be used to guide the clinical margin design of target volumes.

Some reports performed a similar experiment, but they focused on comparing the dosimetric results inside GTV regions,[23,24] instead of the MD region reported in this study. Another report considered the influence of motion-affected dose to the target outline, but they used only 3DCT for dose calculation and would be less accurate.[25] Limitations of this study were that we assumed a rigid motion model and did not take into account the deformation of anatomical structures due to motion. Only the MD region along the SI movement direction was considered. No actual patient respiratory waveforms and no noncoplanar plans were studied. Some breathing patterns could be irregular. IMRT could have an additional effect on the dosimetry in the MD region. However, the interplay effect was not addressed in this study as conformal beams were used. Further investigations are warranted to understand the impacts of these factors on the MD dosimetry.

Conclusions

The use of static dose calculation in the TPS could substantially underestimate the actually delivered dose in the MD region for a moving target. Respiratory movement caused inadvertent irradiation exposure, with 70% to 80% of the dose line wrapped around the 10 mm region outside the target. The conventional margin for MD could be substantially reduced or potentially be eliminated for lung SBRT.

Declaration of Conflicting Interests

The author(s) declared no potential conflicts of interest with respect to the research, authorship, and/or publication of this article.

Funding

The author(s) disclosed receipt of the following financial support for the research, authorship, and/or publication of this article: This research was funded by the National Natural Science Foundation of China 81372436, The Innovation team of Zhengzhou 121PCXTD524, The Ministry of Health, and Henan Province Health Department 201201009.

References

1. Chui CS, Yorke E, Hong L. The effects of intra-fraction organ motion on the delivery of intensity-modulated field with a multileaf collimator. *Med Phys*. 2003;30(7):1736-1746.
2. Ge Y, O'Brien RT, Shieh CC, Booth JT, Keall PJ. Toward the development of intrafraction tumor deformation tracking using a dynamic multi-leaf collimator. *Med Phys*. 2014;41(6):061703.
3. Rosenzweig KE, Hanley J, Mah D, et al. The deep inspiration breath-hold technique in the treatment of inoperable non-small-cell lung cancer. *Int J Radiat Oncol Biol Phys*. 2000;48(1):81-87.
4. Dietrich L, Tucking T, Nill S, Oelfke U. Compensation for respiratory motion by gated radiotherapy: an experimental study. *Phys Med Biol*. 2005;50(10):2405-2414.

5. Nelson C, Starkschall G, Balter P, et al. Respiration-correlated treatment delivery using feedback-guided breath hold: a technical study. *Med Phys*. 2005;32(1):175-181.
6. Zhang T, Orton NP, Tome WA. On the automated definition of mobile target volumes from 4D-CT images for stereotactic body radiotherapy. *Med Phys*. 2005;32(11):3493-3502.
7. Rietzel E, Chen GT, Choi NC, Willet CG. Four-dimensional image-based treatment planning: target volume segmentation and dose calculation in the presence of respiratory motion. *Int J Radiat Oncol Biol Phys*. 2005;61(5):1535-1550.
8. George R, Vedam SS, Chung TD, Ramakrishnan V, Keall PJ. The application of the sinusoidal model to lung cancer patient respiratory motion. *Med Phys*. 2005;32(9):2850-2861.
9. Klein M, Gaede S, Yartsev S. A study of longitudinal tumor motion in helical tomotherapy using a cylindrical phantom. *J Appl Clin Med Phys*. 2013;14(2):4022.
10. Lujan AE, Larsen EW, Balter JM, Ten Haken RK. A method for incorporating organ motion due to breathing into 3D dose calculations. *Med Phys*. 1999;26(5):715-720.
11. Fuss M, Sturtewagen E, De Wagter C, Georg D. Dosimetric characterization of GafChromic EBT film and its implication on film dosimetry quality assurance. *Phys Med Biol*. 2007;52(14): 4211-4225.
12. Zhang Y, Yin FF, Ren L. Dosimetric verification of lung cancer treatment using the CBCTs estimated from limited-angle on-board projections. *Med Phys*. 2015;42(8):4783-4795.
13. Saur S, Frengen J. GafChromic EBT film dosimetry with flatbed CCD scanner: a novel background correction method and full dose uncertainty analysis. *Med Phys*. 2008;35(7):3094-3101.
14. Giraud P, Antoine M, Larrouy A, et al. Evaluation of microscopic tumor extension in non-small-cell lung cancer for three dimensional conformal radiotherapy planning. *Int J Radiat Oncol Biol Phys*. 2000;48(4):1015-1024.
15. Grills IS, Yan D, Black QC, Wong CY, Martinez AA, Kestin LL. Clinical implications of defining the gross tumor volume with combination of CT and ^{18}FDG-positron emission tomography in non-small-cell lung cancer. *Int J Radiat Oncol Biol Phys*. 2007; 67(3):709-719.
16. Morarji K, Fowler A, Vinod SK, Ho Shon I, Laurence JM. Impact of FDG-PET on lung cancer delineation for radiotherapy. *J Med Imaging Radiat Oncol*. 2012;56(2):195-203.
17. Ge H, Cai J, Kelsey CR, Yin FF. Quantification and minimization of uncertainties of internal target volume for stereotactic body radiation therapy of lung cancer. *Int J Radiat Oncol Bio Phys*. 2013;85(2):438-443.
18. Yuan S, Meng X, Yu J, et al. Determining optimal clinical target volume margins on the basis of microscopic extracapsular extension of metastatic nodes in patients with non-small-cell lung cancer. *Int J Radiat Oncol Biol Phys*. 2007;67(3):727-734.
19. Grills IS, Fitch DL, Goldstein NS, et al. Clinicopathologic analysis of microscopic extension in lung adenocarcinoma: defining clinical target volume for radiotherapy. *Int J Radiat Oncol Biol Phys*. 2007;69(2):334-341.
20. Dewas S, Bibault JE, Blanchard P, et al. Delineation in thoracic oncology: a prospective study of the effect of training on contour variability and dosimetric consequences. *Radiat Oncol*. 2011;6:118.
21. ICRU. International Commission on Radiation Units and Measurements. "Prescribing, Recording and Reporting Photon Beam Therapy" (Supplement to ICRU Report 50). ICRU Report 62,1999 (International Commission on Radiation Units and Measurements, Bethesda, MD).
22. Withers HR, Peters LJ, Taylor JM. Dose–response relationship for radiation therapy of subclinical disease. *Int J Radiat Oncol Biol Phys*. 1995;31(2):353-361.
23. Guckenberger M, Wilbert J, Krieger T, et al. Four-dimensional treatment planning for stereotactic body radiotherapy. *Int J Radiat Oncol Biol Phys*. 2007;69(1):276-285.
24. Vinogradskiy YY, Balter P, Followill DS, Alvarez PE, White RA, Starkschall G. Comparing the accuracy of four-dimensional photon dose calculations with three-dimensional calculations using moving and deforming phantoms. *Med Phys*. 2009; 36(11):5000-5006.
25. Jin JY, Ajlouni M, Kong FM, Ryu S, Chetty IJ, Movsas B. Utilize target motion to cover clinical target volume (CTV)—a novel and practical treatment planning approach to manage respiratory motion. *Radiother Oncol*. 2008;89(3):292-303.